

Journal of
***Mechanics of
Materials and Structures***

**BOUNDARY ELEMENT ANALYSIS OF THE STRESS FIELD AT
THE SINGULARITY LINES IN THREE-DIMENSIONAL BONDED
JOINTS UNDER THERMAL LOADING**

Monchai Prukvilailert and Hideo Koguchi

Volume 2, N° 1

January 2007

BOUNDARY ELEMENT ANALYSIS OF THE STRESS FIELD AT THE SINGULARITY LINES IN THREE-DIMENSIONAL BONDED JOINTS UNDER THERMAL LOADING

MONCHAI PRUKVILAILERT AND HIDEO KOGUCHI

The stress distribution near a point on the stress singularity line of dissimilar materials in three-dimensional joints under thermal loading are investigated using BEM based on Rongved's fundamental solutions. Stress distributions for the material combinations in the singularity region, in the no singularity region, and in the boundary between them on the Dundurs composite plane are investigated. The influences of thermal expansion coefficients, loading conditions and dimensions on the stress distribution in three-dimensional joints composed of two blocks are examined. The stress intensity factors in three-dimensional joints under a uniform change in temperature are proportional to the temperature variation, ΔT , and depend on the difference in the thermal expansion coefficients. Furthermore, the level of the stress distributions around the stress singularity lines also increases significantly as the length of one side in the parallel cross section to the interface decreases.

1. Introduction

Stress singularities at the interface in the bonded joints of dissimilar materials are induced by mechanical loading or thermal loading. Thermal stresses are caused by differences in elastic properties and thermal expansion coefficients in dissimilar materials joints. The stress singularities exist not only at the vertex in three-dimensional joints of dissimilar materials but also along the intersection of the interface with its free surfaces. The cross line has been referred to as the stress singularity line. Li et al. [1992] reported the results of stress analysis for dissimilar materials using three-dimensional BEM based on Kelvin's fundamental solutions. In the analysis, the interface must be divided using very fine meshes along the stress singularity lines, and hugely memory- and time-consuming procedures are required for accurate analysis. Then, Koguchi [1997] investigated the stress singularity in three-dimensional bonded joints using three-dimensional BEM based on Rongved's fundamental solutions. Rongved's fundamental solutions [Rongved 1955] satisfy boundary conditions at the interface. Therefore, the number of nodes and elements necessary for accurate analysis decreases, because the BEM based on Rongved's fundamental solutions does not require the interface area of dissimilar materials joints to be divided into elements. Koguchi et al. [2003] also used the fundamental solution for two-phase transversely isotropic materials to investigate the stress singularity fields in three-dimensional bonded joints using three-dimensional BEM. Furthermore, Prukvilailert and Koguchi [2005] reported on stress singularity analysis around a point on the stress singularity line in three-dimensional bonded joints using three-dimensional BEM based on Rongved's fundamental solutions. However, this previous research focused only on the stress

Keywords: thermoelasticity, thermal stress, logarithmic singularity, stress singularity, three-dimensional joints, dissimilar materials, BEM.

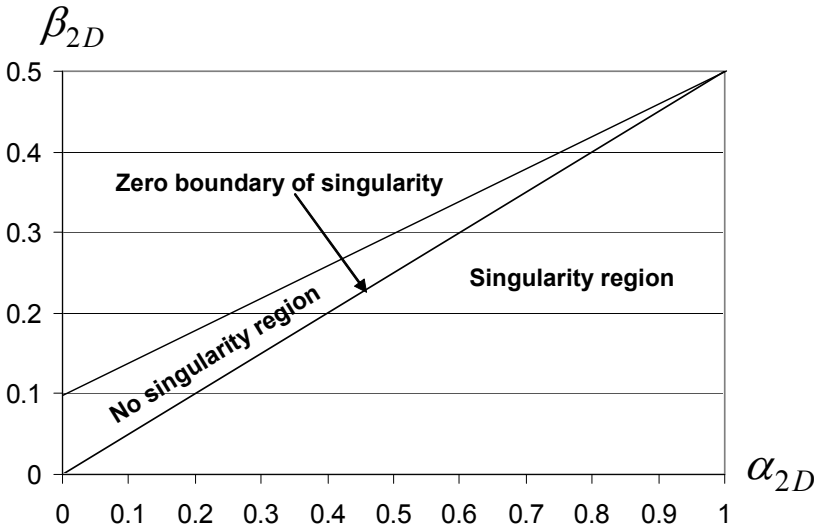


Figure 1. The Dundurs composite plane.

singularity distributions in three-dimensional bonded joints under mechanical loading. The distributions of the stress fields near the point on the stress singularity line in three-dimensional joints of dissimilar materials under thermal loading have not been made clear so far.

In recent years, there has been much research on thermal stresses at the interface in two-dimensional bonded joints. Munz and Yang [1992], Munz and Yang [1994] and Yang and Munz [1995] investigated the stress singularities and stress intensity factors near the free edge of a junction between dissimilar materials subjected to mechanical or thermal loading using the eigenfunction expansion method. Madenci et al. [1998] and Barut et al. [2001] developed global (special) elements in a finite element analysis to investigate the thermo-mechanical stress field in a junction between dissimilar materials. It is well-known that three-dimensional BEM is useful to efficiently analyze the stress fields in three-dimensional joints, since only surfaces are divided into meshes for analysis. Cruse et al. [1977] and Rizzo and Shippy [1977] determined the boundary integral equation for three-dimensional thermoelasticity. The thermoelastic integral equation was also derived using the body force analogy [Karami and Kuhn 1992; Cheng et al. 2001].

In this paper, we investigate the stress singularity fields near the singular point on the stress singularity line in three-dimensional joints of dissimilar materials under thermal loading using BEM based on Rongved's fundamental solutions. The material combinations are mapped on the $\alpha_{2D} - \beta_{2D}$ Dundurs composite plane [1969] for the order of stress singularity in a form of power-law singularity, λ_a , in plane strain condition as shown in Figure 1. These parameters are defined as:

$$\alpha_{2D} = \frac{K m_{(2)} - m_{(1)}}{K m_{(2)} + m_{(1)}}, \quad (1)$$

$$\beta_{2D} = \frac{K(m_{(2)} - 2) - (m_{(1)} - 2)}{K m_{(2)} + m_{(1)}},$$

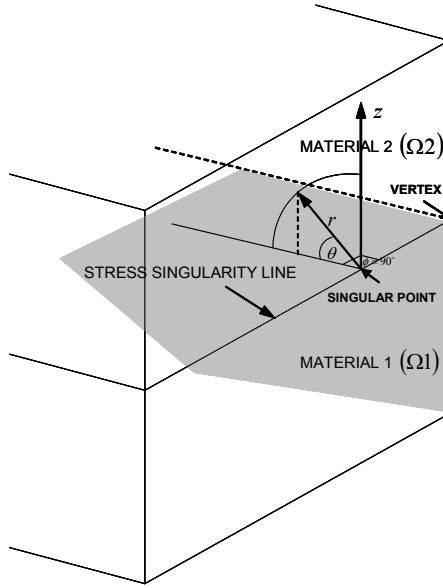


Figure 2. Stress singularity line in a three-dimensional joint of dissimilar materials and spherical coordinate system with the origin at the singular point.

where

$$K = \frac{G_{(1)}}{G_{(2)}}, \quad (2)$$

$$m_{(h)} = \begin{cases} 4(1 - v_{(h)}), & \text{for plane strain,} \\ \frac{4}{1 + v_{(h)}}, & \text{for plane stress,} \end{cases} \quad (h = 1, 2) \quad (3)$$

in which $G_{(h)}$ is the shear modulus and $v_{(h)}$ is the Poisson's ratio. The subscript h of these material properties represents the material region; subscript 1 refers to the region of material 1 and subscript 2 refers to the region of material 2. Prukvilailert and Koguchi [2005] investigated the eigenvalues for the point on the stress singularity line in three-dimensional bonded joints using the formulation of FEM eigen analysis developed by Yamada and Okumura [1981] and Pageau and Biggers [1995]. The eigen equation was derived using the principles of virtual work for deducing the root p (eigenvalue). We obtained quintuple roots ($p_l = 1$) of logarithmic singularity and a root p_a where $0 < p_a < 1$ of r^{λ_a} power-law singularity. We found that the order of stress singularity in a form of power-law singularity, λ_a ($\lambda_a = p_a - 1$), at the point on the stress singularity line, is almost identical to that at the apex of two-dimensional bonded joints in plane strain condition, and the contour map of λ_a in the singular region of the Dundurs composite plane was plotted. The stress singularity field around the singular point on the stress singularity line according to the eigenvalues obtained by three-dimensional FEM eigen analysis can be expressed as follows:

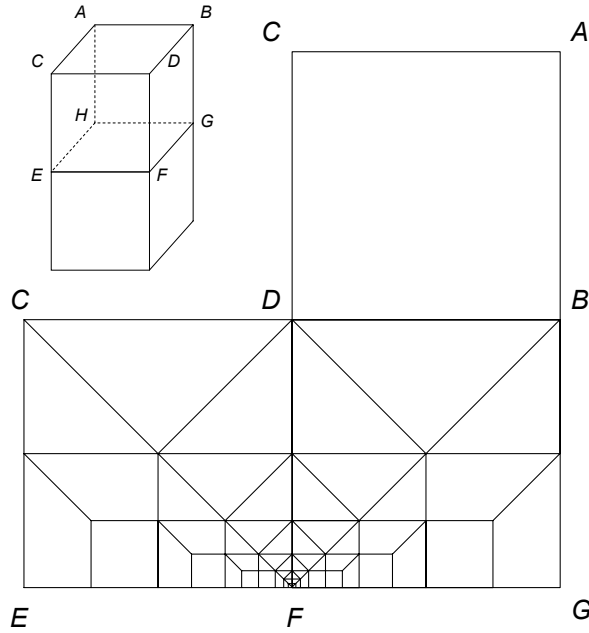


Figure 3. Mesh division of the model.

$$\begin{aligned} \sigma_{ij}(r, \theta, \phi) = & L_{ij1}(\theta, \phi) + L_{ij2}(\theta, \phi) \ln(r/L) + L_{ij3}(\theta, \phi) (\ln(r/L))^2 \\ & + L_{ij4}(\theta, \phi) (\ln(r/L))^3 + L_{ij5}(\theta, \phi) (\ln(r/L))^4 + (r/L)^{\lambda_a} K_{ija}(\theta, \phi, p_a), \end{aligned} \quad (4)$$

where L is the characteristic length of the configuration. L_{ijm} is the stress intensity factor of the logarithmic singularity term ($m = 1, 2, \dots, 5$), and K_{ija} is that of the $(r/L)^{\lambda_a}$ term. The subscripts i, j refer to r, θ and ϕ in a spherical coordinate system as shown in Figure 2.

2. BEM for thermoelasticity

The stress and displacement fields at a point in the joints with high stress are examined using BEM, which requires less memory than FEM, especially in the case of three-dimensional joints. Here, Rongved's fundamental solutions satisfying the boundary conditions at the interface in dissimilar materials are applied in our analysis. For thermoelasticity with a uniform temperature variation in dissimilar materials, the boundary integral equation is derived as follows:

$$C_{ij}u_j(P) = \int_S (t_j(Q)U_{ij}(P, Q) - T_{ij}(P, Q)u_j(Q))dS(Q) + \int_S ((n_j M \varphi)U_{ij}(P, Q))dS(Q), \quad (5)$$

where S is the surface of the dissimilar materials model excluding the interface area, P and Q are points on the boundary, C_{ij} is the C -matrix derived from the configuration around a boundary point P , and U_{ij} and T_{ij} are Rongved's fundamental solutions for displacements and surface tractions. Parameter φ is a uniform temperature variation from the stress-free state. The term M varies according to the location of

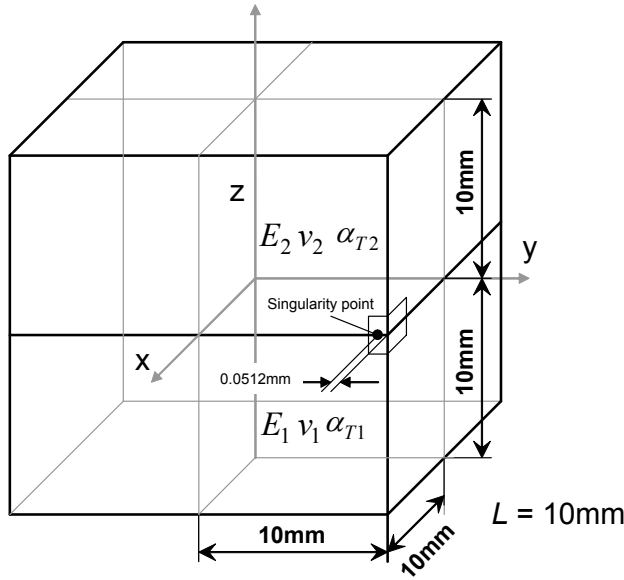


Figure 4. Model for analysis of a three-dimensional joint.

an element. We can define M as

$$M = \begin{cases} \frac{2G_{(1)}\alpha_{T1}(1+v_{(1)})}{(1-2v_{(1)})}, & \text{in Material region 1,} \\ \frac{2G_{(2)}\alpha_{T2}(1+v_{(2)})}{(1-2v_{(2)})}, & \text{in Material region 2,} \end{cases} \quad (6)$$

where α_{T1} and α_{T2} are the thermal expansion coefficients for material 1 and for material 2, respectively.

A very fine mesh division shown in Figure 3 is used to obtain an accurate stress distribution. The stress state at internal points can then be derived. First, the strain-displacement relation is written as

$$\varepsilon_{ij} = \frac{1}{2}(u_{i,j} + u_{j,i}). \quad (7)$$

The stress-strain relation for thermoelasticity is given by

$$\sigma_{ij}^{(h)} = 2G^{(h)}\varepsilon_{ij} + N\delta_{ij}\varepsilon_{kk} - M\delta_{ij}\varphi, \quad (8)$$

where

$$N = \begin{cases} \frac{2G_{(1)}v_{(1)}}{(1-2v_{(1)})}, & \text{in material region 1,} \\ \frac{2G_{(2)}v_{(2)}}{(1-2v_{(2)})}, & \text{in material region 2.} \end{cases} \quad (9)$$

Substitution of Equation (7) into Equation (8) then gives

$$\sigma_{ij}^{(h)} = G^{(h)}(u_{i,j} + u_{j,i}) + N\delta_{ij}u_{k,k} - M\delta_{ij}\varphi. \quad (10)$$

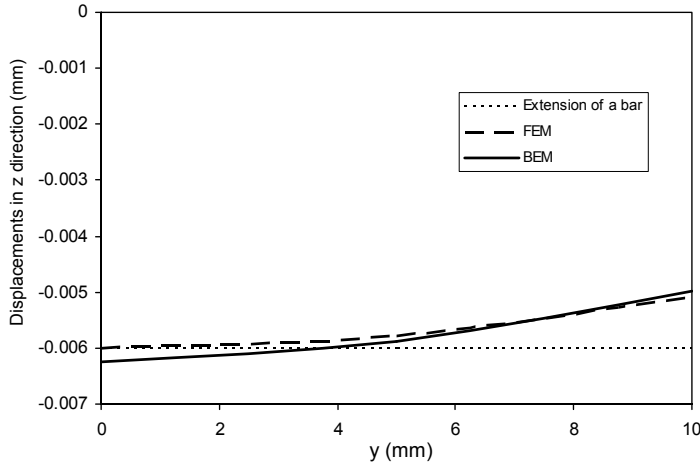


Figure 5. Displacements in the z -direction on the upper surface of the model along the edge $x = 10$ mm for a uniform temperature variation ($\Delta T = -100$ K, cooling down).

Finally, the stress σ_{ij} at the internal point, ξ , can be obtained by differentiating Equation (5) and substituting into Equation (10) as follows:

$$\sigma_{ij}^{(h)}(\xi) = \int_S \left(t_l(Q) D_{ijl}^{(h)}(\xi, Q) - V_{ijl}^{(h)}(\xi, Q) u_l(Q) \right) dS(Q) + \int_S \left(n_l M \varphi \right) D_{ijl}^{(h)}(\xi, Q) dS(Q) - M \delta_{ij} \varphi, \quad (11)$$

where the third-order tensor components $D_{ijl}^{(h)}(\xi, Q)$ and $V_{ijl}^{(h)}(\xi, Q)$ are obtained by substituting Rongved's fundamental solutions $U_{ij}(\xi, Q)$ and $T_{ij}(\xi, Q)$, respectively, in the stress-displacement equations as follows:

$$\begin{aligned} D_{ijl}^{(h)}(\xi, Q) &= G_{(h)} \left(U_{il,j}(\xi, Q) + U_{jl,i}(\xi, Q) \right) + N \delta_{ij} U_{kl,k}(\xi, Q) \\ V_{ijl}^{(h)}(\xi, Q) &= G_{(h)} \left(T_{il,j}(\xi, Q) + T_{jl,i}(\xi, Q) \right) + N \delta_{ij} T_{kl,k}(\xi, Q), \end{aligned} \quad (12)$$

where δ_{ij} is the Kronecker delta.

A typical model employed in our calculation is shown in Figure 4. The total number of nodes and elements are 3067 and 1370, respectively. A very fine mesh division is located around the singular point on the stress singularity line. For the boundary conditions, the displacements in the x -direction and the y -direction are free at all surfaces of the model. The displacement in the z -direction at the upper surface and side surfaces of the model is free, whereas that at the lower surface is fixed to zero.

3. Results and discussion

3.1. Thermal loading. In this section, thermal loading due to a uniform temperature variation ($\varphi = \Delta T$: constant) is applied to the three-dimensional joint model. The material combinations of the joint are chosen so as to lie in the singularity region, in the no-singularity region and at the boundary between the two; here “singularity” refers to the power-law singularity on the Dundurs composite plane in Figure 1. The

distance between the vertex of the joint and the singular point where the stress distribution is investigated is 0.0512 mm as shown in Figure 4. Material properties are first chosen as $E_{(1)} = 206$ GPa, $\nu_{(1)} = 0.3$, $E_{(2)} = 52.6742$ GPa, $\nu_{(2)} = 0.26316$. The corresponding Dundurs parameters ($\alpha_{2D} = 0.6$, $\beta_{2D} = 0.2$) are in the singularity region. The thermal expansion coefficient of material 1, α_{T1} , is $1.0 \times 10^{-6} K^{-1}$, and of material 2, α_{T2} , it is $5.0 \times 10^{-6} K^{-1}$. The uniform temperature variation ΔT is $-100K$, which means that the temperature in the joint decreases from the stress-free state (ΔT is negative, indicating a cooling-down condition). The upper part of the model (material 2) allows more contraction than the lower part of the model (material 1, which has a lower value of the thermal expansion coefficient). A comparison of the displacements in the z -direction along the edge ($x = 10$ mm) on the upper surface of the model in the BEM analysis with those in the FEM and theoretical analysis is shown in Figure 5. The theoretical analysis based on the theory of thermoelasticity for the extension of a bar shows the average displacement over the upper surface of the model. As seen in Figure 5, the displacements for each of the three methods are close to each other. The results of the BEM and the FEM also show that the displacement varies over the upper surface of the model. The stress distribution of $\sigma_{\theta\theta}$ at the interface ($\theta = 0^\circ$) near the singular point on the stress singularity line along the dimensionless distance r/L in the present BEM analysis for a uniform temperature variation ($\Delta T = -100K$) is shown in Figure 6a. For comparison, we also provide the stress distributions of $\sigma_{\theta\theta}$ in two-dimensional bonded joints, computed using the formulation developed by Munz and Yang [1992] and the commercial FEM program (MARC) in plane strain condition. It can be seen that the stress distribution of $\sigma_{\theta\theta}$ for three-dimensional bonded joints is similar to that for two-dimensional bonded joints, but the magnitude is larger. The stress distributions of $\sigma_{\theta\theta}$ around the singular points located at 0.0392 mm and 0.0292 mm from the junction vertex are also investigated. To magnify the difference, Figure 6b shows the stress distributions of $\sigma_{\theta\theta}$ in a semilog scale for the three singular points. The level of the stress $\sigma_{\theta\theta}$ increases slightly as the singular point approaches the vertex point. Next, the stress distributions of $\sigma_{\theta\theta}$ for various uniform temperature variations are investigated and shown in Figure 7. The magnitude of the stress $\sigma_{\theta\theta}$ near the singular point is proportional to the value of a uniform temperature variation according to the Linear Theory of Elasticity. Figures 8a–8c show the distributions of several stress components $-\sigma_{ij}/\Delta T$ near the singular point in a log-log scale for various angles of θ . The stress level of $-\sigma_{\theta\theta}/\Delta T$ in Figure 8a increases as the angle θ approaches 0.

It is well-known that failure and cracks at the interface of joints usually occur due to the tensile stress of $\sigma_{\theta\theta}$. The stress distribution of $-\sigma_{\theta\theta}/\Delta T$ at $\theta = 0^\circ$ in Figure 8a refers to the stress distribution of $\sigma_{\theta\theta}$ at the interface in Figure 6a divided by $\Delta T = -100K$. Moreover, the stress level of $-\sigma_{r\theta}/\Delta T$ in Figure 8b decreases while the stress level of $-\sigma_{rr}/\Delta T$ in Figure 8c increases as the angle θ approaches the free surface of joints. The stress components computed at $\theta = -10^\circ$, -30° and -60° are not reported in the corresponding figures since their values are negative. All plots obviously have negative slopes. Therefore, the occurrence of stress singularity in the form of $(r/L)^{\lambda_a}$ singularity (power-law singularity) is possible. However, the curves deviate from a straight line as the distance from the singular point increases. An attempt to estimate the stress distribution using a function of the 1st order logarithmic singularity term and the power-law singularity term for two-dimensional joints does not provide a good fit for the stress distribution of $-\sigma_{\theta\theta}/\Delta T$ at $\theta = -60^\circ$ shown in Figure 8a. In the present study, three-dimensional FEM eigen analysis yields one root of power-law singularity, $p_a = 0.9073$, $\lambda_a = p_a - 1 = -0.0927$, and quintuple roots ($p_l = 1$) of logarithmic singularity. Then, a good fit for the profiles of the stress

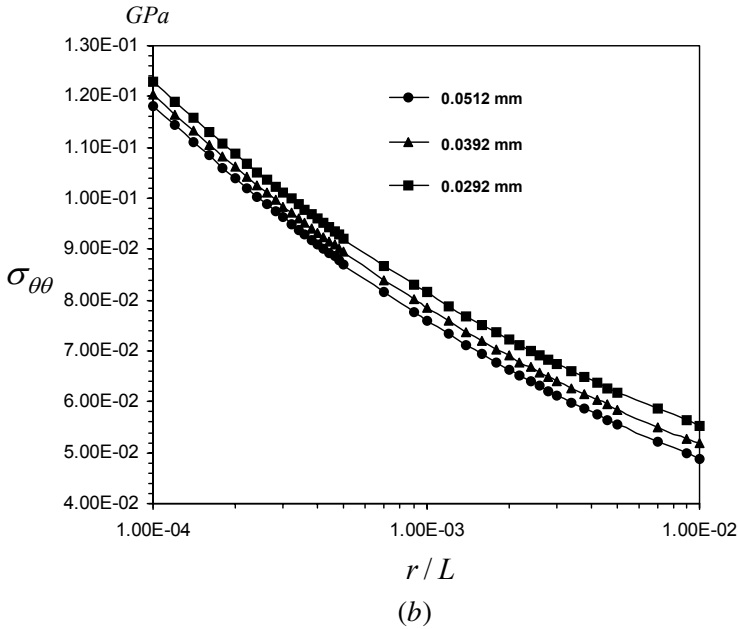
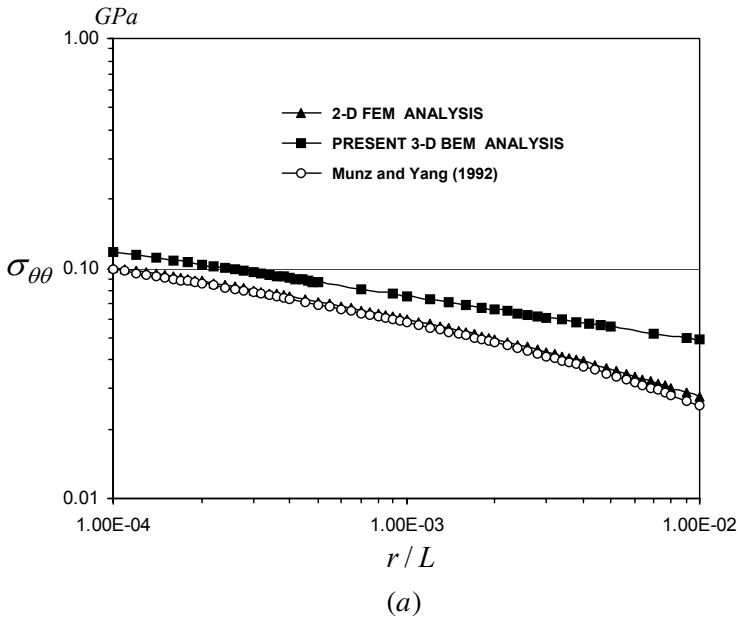


Figure 6. Stress distributions of $\sigma_{\theta\theta}$ at the interface near the singular point on the stress singularity line for a uniform temperature variation ($\Delta T = -100$ K).

distributions in the neighborhood of the singular point can be obtained using Equation (4) which is a combination of power-law singularity and 4th order logarithmic singularity distributions. Figure 9a shows the stress distributions of $-\sigma_{\theta\theta}/\Delta T$ at the interface ($\theta = 0^\circ$) for various values of α_{T2} when α_{T1} is fixed to $1.0 \times 10^{-6} K^{-1}$. The stress level of $-\sigma_{\theta\theta}/\Delta T$ increases as the value of α_{T2} increases.

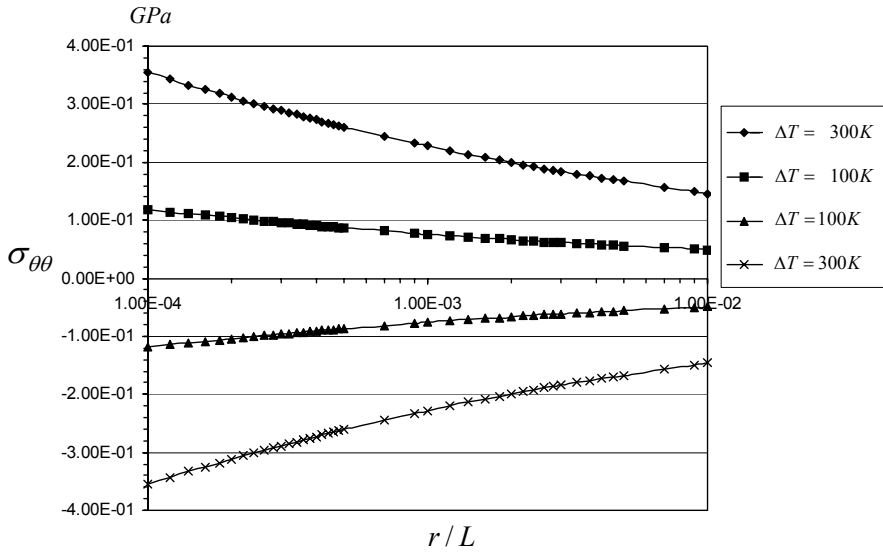
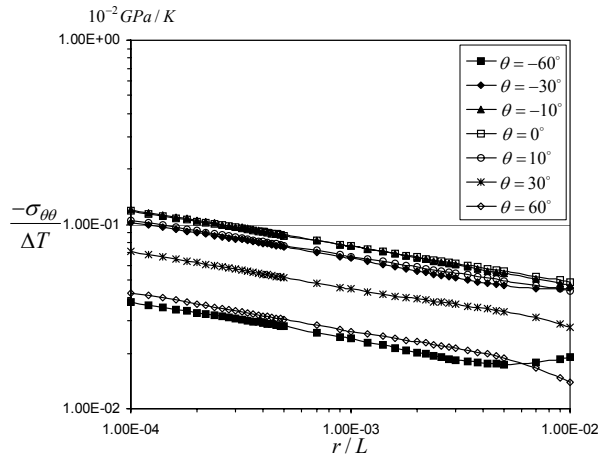
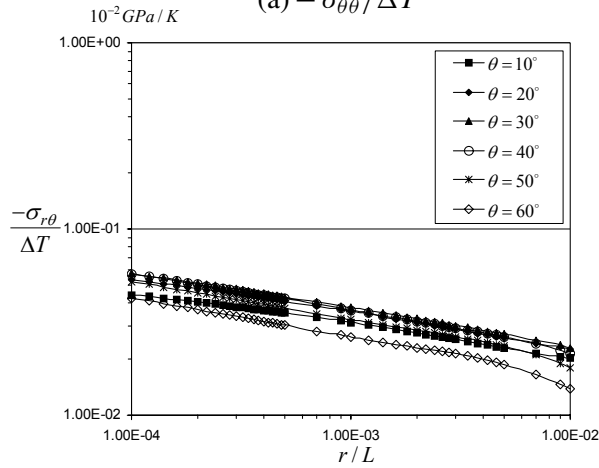


Figure 7. Stress distributions of $\sigma_{\theta\theta}$ at the interface for various uniform temperature variations in a semilog scale.

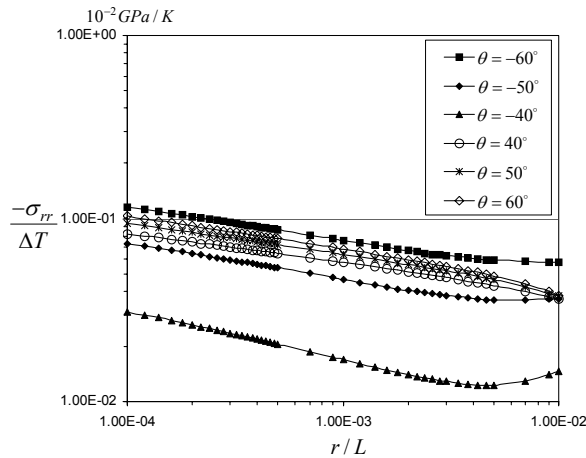
Furthermore, Figure 9b shows that the stress field is linear in the difference between the thermal expansion coefficients. Figures 10a–10c show the log-log plots of $-\sigma_{ij}/\Delta T$ for various angles of θ and the Dundurs parameters located at the zero boundary of singularity in plane strain condition ($\alpha_{2D} = 0.4$, $\beta_{2D} = 0.2$, $E_{(1)} = 206$ GPa, $\nu_{(1)} = 0.3$, $E_{(2)} = 94.68124$ GPa, $\nu_{(2)} = 0.15517$). The thermal expansion coefficients for two dissimilar materials are chosen as $\alpha_{T1} = 1.0 \times 10^{-6} K^{-1}$ and $\alpha_{T2} = 5.0 \times 10^{-6} K^{-1}$. From the three-dimensional FEM eigen value analysis, there are five roots of $p_l = 1$ and $\lambda_a = -0.000455$. We also used Equation (4) to approximate the curves of the stress distributions. Because of the very small order of stress singularity ($\lambda_a \rightarrow 0$), the $(r/L)^{\lambda_a}$ singularity term in Equation (4) is almost constant in the range $10^{-4} \leq r/L \leq 10^{-2}$. However, in Figure 10a, the plots of the stress $-\sigma_{\theta\theta}/\Delta T$ have significantly negative slopes. The plots for the stresses $-\sigma_{r\theta}/\Delta T$ and $-\sigma_{rr}/\Delta T$ in Figure 10b–10c also have negative slopes. This means that the existence of logarithmic singularity clearly influences the characteristics of the stress fields near the stress singularity line for material combinations at the zero boundary of singularity on the Dundurs composite plane. We also investigate the stress distributions of $-\sigma_{ij}/\Delta T$ for the Dundurs parameters located in the no-singularity region ($\alpha_{2D} = 0.3$, $\beta_{2D} = 0.2$, $E_{(1)} = 206$ GPa, $\nu_{(1)} = 0.3$, $E_{(2)} = 121.2716$ GPa, $\nu_{(2)} = 0.07143$, $\lambda_a = 0.02752 > 0$). It can be found that the characteristics of the stress distributions of $-\sigma_{ij}/\Delta T$ are similar to those at the zero boundary of singularity, because the Dundurs parameters in the two cases are not very different. The stress distributions of $-\sigma_{\theta\theta}/\Delta T$ at the interface for material combinations falling in the no-singularity region and at the zero boundary of singularity when the difference of the thermal coefficient is varied are shown in Figure 11. The stress distributions for material combinations in the singularity region, in the no-singularity region, and at the zero boundary of singularity show that the stress intensity factors in Equation (4) are proportional to the temperature variation ΔT and depend on the difference in the thermal expansion coefficients in



(a) $-\sigma_{\theta\theta}/\Delta T$

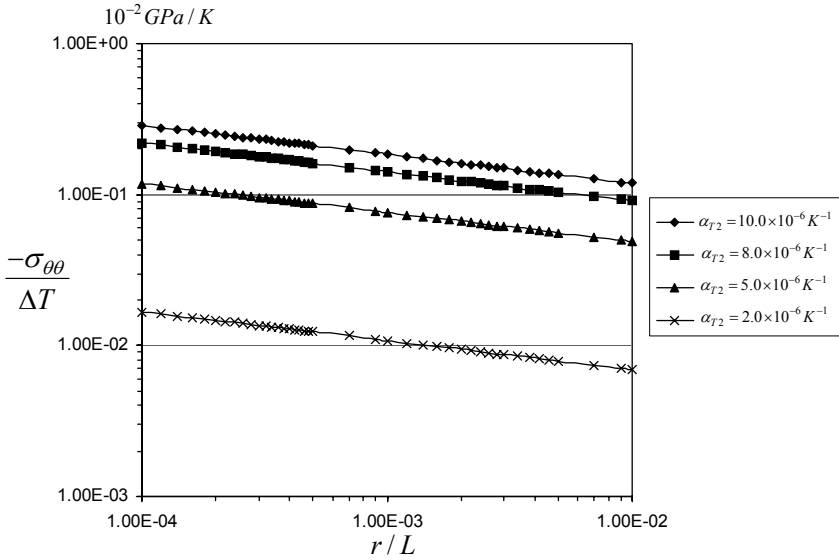


(b) $-\sigma_{r\theta}/\Delta T$

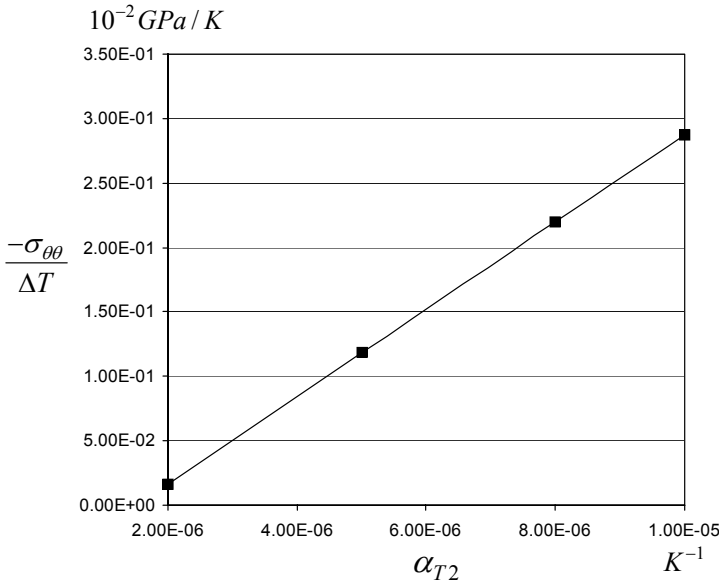


(c) $-\sigma_{rr}/\Delta T$

Figure 8. Stress distributions of $-\sigma_{ij}/\Delta T$ for various angles of θ ($\alpha_{2D} = 0.6$, $\beta_{2D} = 0.2$).



(a)



(b)

Figure 9. Stress distributions of $-\sigma_{\theta\theta}/\Delta T$ at the interface $\theta = 0^\circ$ for various values of α_{T2} ($\alpha_{T1} = 1.0 \times 10^{-6} K^{-1}$ and $\alpha_{2D} = 0.6, \beta_{2D} = 0.2$).

two-phase materials, that is,

$$L_{ijm} \quad \text{and} \quad K_{ija} \propto \Delta T. \tag{13}$$

The stress intensity factors for the stress $-\sigma_{\theta\theta}/\Delta T$ at the interface under a uniform temperature variation are shown in Table 1. The stress intensity factors $-L_{\theta\theta 4}/\Delta T$ and $-L_{\theta\theta 5}/\Delta T$ are relatively

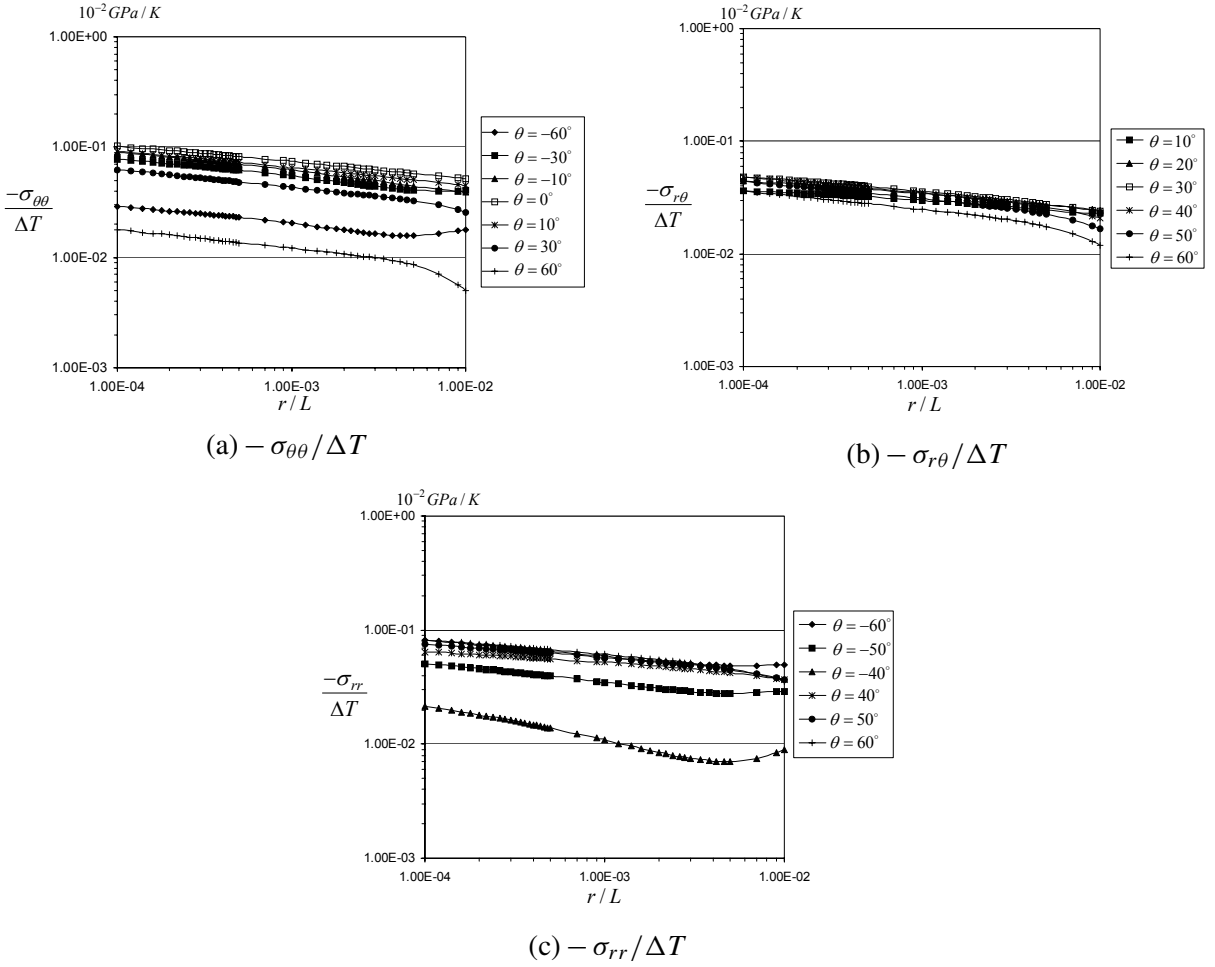


Figure 10. Stress distributions of $-\sigma_{\theta\theta}/\Delta T$ for various angles of θ ($\alpha_{2D} = 0.4, \beta_{2D} = 0.2$).

	$-K_{\theta\theta a}/\Delta T$ 10^{-2} GPa/K	$-L_{\theta\theta 1}/\Delta T$ 10^{-2} GPa/K	$-L_{\theta\theta 2}/\Delta T$ 10^{-2} GPa/K	$-L_{\theta\theta 3}/\Delta T$ 10^{-2} GPa/K	$-L_{\theta\theta 4}/\Delta T$ 10^{-2} GPa/K	$-L_{\theta\theta 5}/\Delta T$ 10^{-2} GPa/K
$\alpha_{2D} = 0.6, \beta_{2D} = 0.2$ $\lambda = -0.0927$	4.233E-02	-5.381E-03	7.210E-03	1.072E-03	1.263E-06	8.683E-08
$\alpha_{2D} = 0.5, \beta_{2D} = 0.2$ $\lambda = -0.000455$	7.663E-02	-5.510E-02	-4.173E-03	4.575E-04	-1.015E-05	-6.968E-07
$\alpha_{2D} = 0.3, \beta_{2D} = 0.2$ $\lambda = -0.02752$	8.490E-02	-6.879E-02	-8.646E-03	1.069E-04	-1.382E-05	-9.482E-07

Table 1. Stress intensity factors for the stress $-\sigma_{\theta\theta}/\Delta T$ at the interface ($\theta = 0$) under a uniform temperature variation. Note: $\alpha_{T1} = 1.0 \times 10^{-6} K^{-1}, \alpha_{T2} = 5.0 \times 10^{-6} K^{-1}$.

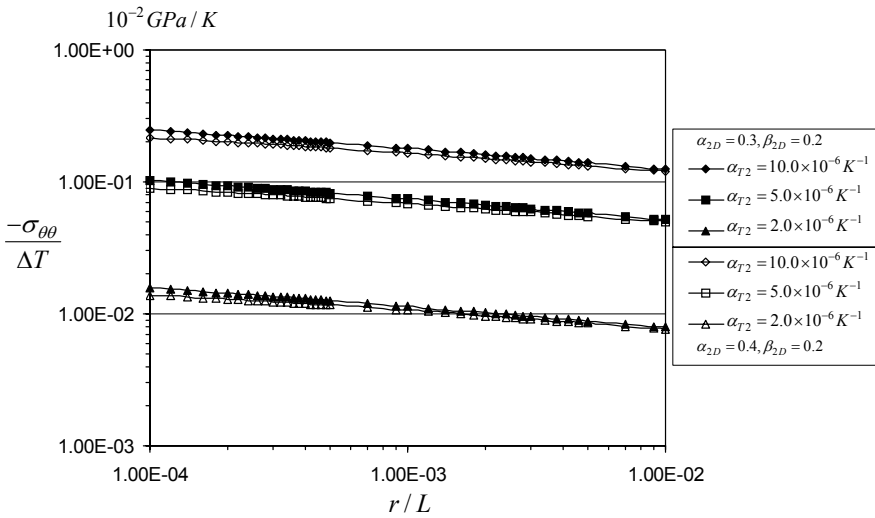


Figure 11. Effects of α_{T2} ($\alpha_{T1} 1.0 \times 10^{-6} K^{-1}$) on $\sigma_{\theta\theta}/\Delta T$ at the interface $\theta = 0$ for ($\alpha_{2D} = 0.4, \beta_{2D} = 0.2$) and ($\alpha_{2D} = 0.3, \beta_{2D} = 0.2$).

small compared with other stress intensity factors. For $\alpha_{2D} = 0.6$ and $\beta_{2D} = 0.2$ (singularity region), the stress intensity factor $-K_{\theta\theta a}/\Delta T$ of the $(r/L)^{\lambda_a}$ singularity term is obviously larger than that for

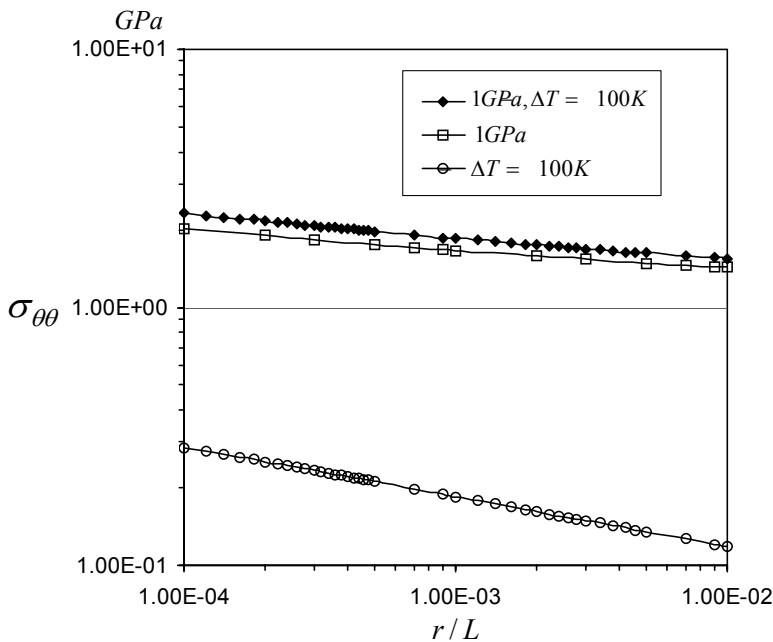


Figure 12. Stress distributions of $\sigma_{\theta\theta}$ at the interface near the singular point on the stress singularity line under various loading conditions.

each of the logarithmic singularity terms. For $(\alpha_{2D} = 0.4, \beta_{2D} = 0.2)$ and $(\alpha_{2D} = 0.3, \beta_{2D} = 0.2)$, it can be seen that the plots of the stress $-\sigma_{\theta\theta}/\Delta T$ against the dimensionless distance r/L in a log-log scale have significantly negative slopes due to the value of the stress intensity factors $-L_{\theta\theta 2}/\Delta T$ of the $\ln(r/L)$ term and $-L_{\theta\theta 3}/\Delta T$ of the $(\ln(r/L))^2$ term in Equation (4). In previous papers [Koguchi 1997; Prukvilailert and Koguchi 2005], it was found that the stress intensity factors (L_{ijm}, K_{ija}) under tensile loading are proportional to the magnitude of the applied tensile stress, P , on the upper surface of three-dimensional joints, that is,

$$L_{ijm} \quad \text{and} \quad K_{ija} \propto P. \tag{14}$$

For comparison, the stress distributions of $\sigma_{\theta\theta}$ under tensile loading ($P = 1 \text{ GPa}$) and under combined loading of tensile ($P = 1 \text{ GPa}$) and thermal loading ($\Delta T = -100\text{K}$) are also provided in Figure 12. It can be seen that the characteristic of the stress distribution of $\sigma_{\theta\theta}$ under a uniform temperature variation is different from that under tensile loading or combined loading. For combined loading, the stress level of $\sigma_{\theta\theta}$ increases with decreasing temperature from the stress-free state (cooling down).

3.2. Plate structure. Plate structures composed of dissimilar materials bonded together have many applications in solid mechanics. The stress distributions near the singular point on the stress singularity line of plate structures under thermal loading are investigated in this section. The geometry of the three-dimensional structure in Figure 4 is changed to a plate structure. Figure 13 shows the model for analysis. The width of the $y - z$ plane, $2w$, is varied. Two stress singularity lines exist for examination in this structure. One stress singularity line is located on the $y - z$ plane and another on the $x - z$ plane. The

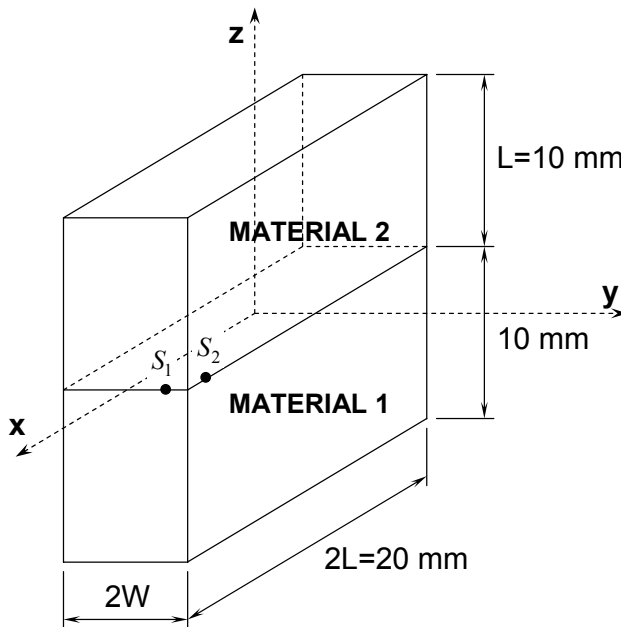


Figure 13. Model for analysis of a plate structure.

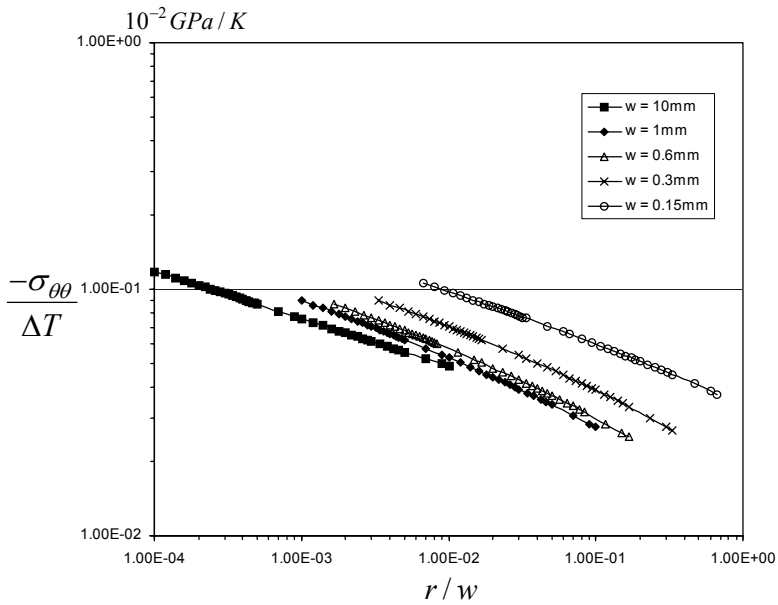


Figure 14. Stress distributions $-\sigma_{\theta\theta}/\Delta T$ around the singular point S_1 at the interface of plate structures.

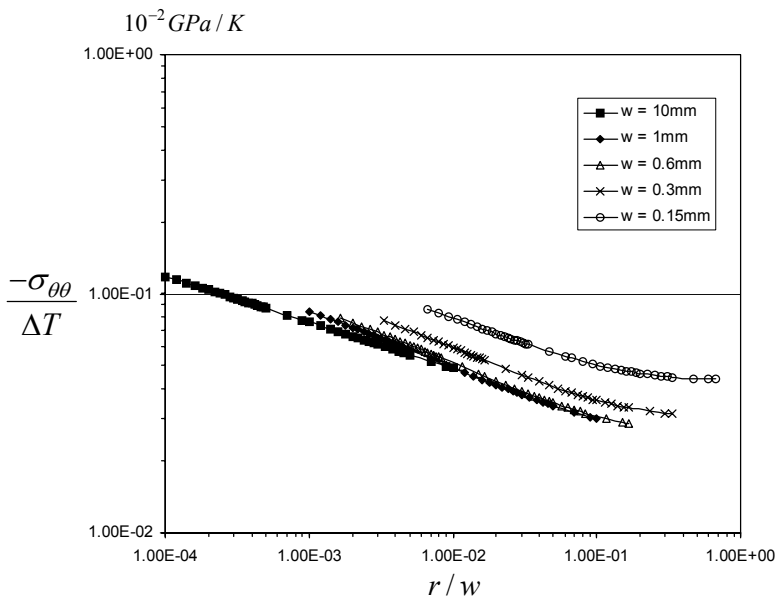


Figure 15. Stress distributions $-\sigma_{\theta\theta}/\Delta T$ around the singular point S_2 at the interface of plate structures.

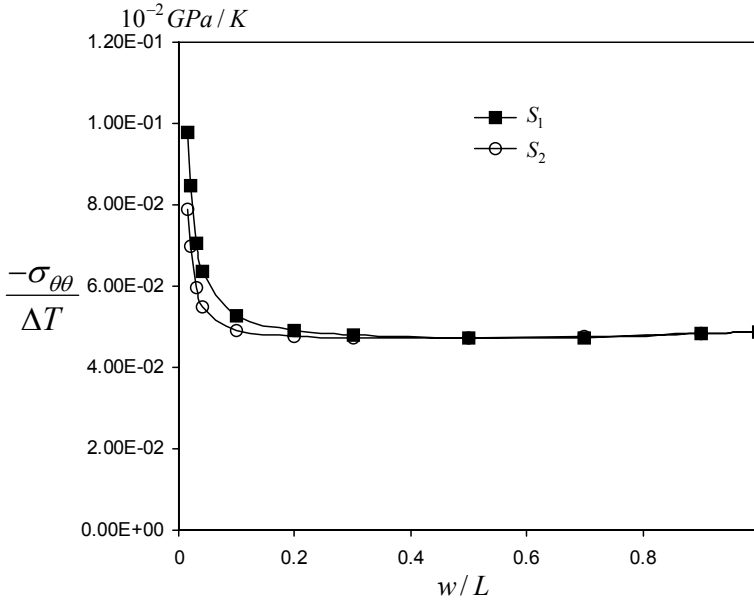


Figure 16. Variation in the stress $-\sigma_{\theta\theta}/\Delta T$ at the interface against the dimensionless variable, w/L , in plate structures.

distance between the singular points (S_1 and S_2) and the vertex of the joint is 0.0512 mm. The material properties are chosen for material combinations corresponding to $\alpha_{2D} = 0.6$ and $\beta_{2D} = 0.2$ (singularity region). The thermal expansion coefficients are chosen as $\alpha_{T1} = 1.0 \times 10^{-6} K^{-1}$ and $\alpha_{T2} = 5.0 \times 10^{-6} K^{-1}$. The temperature variation is uniformly applied to the material regions. Figures 14 and 15 show the stress distributions of $-\sigma_{\theta\theta}/\Delta T$ at the interface around the singular points S_1 and S_2 , respectively, against the dimensionless distance, r/w . The width, w , is varied from 10 mm to 0.15 mm. For the width w from 10 mm to 4 mm, we found that the plots are almost the same line. However, as the width w gets smaller (from 1 mm to 0.15 mm), the plots are clearly different from each other. Because the singular point S_1 is near the singular point S_2 , the characteristics of the stress distributions of $-\sigma_{\theta\theta}/\Delta T$ around the two singular points at the interface are not very different from each other. It can be seen that the dimensionless distance, r/w , is an appropriate variable to determine the variations of the stress distributions around both singular points S_1 and S_2 in plate structures. Therefore, the characteristic length L in Equation (4) is replaced by the width w for the expression of the stress fields around the singular point on the stress singularity line in a plate structure.

Furthermore, the variations in the magnitude of the stress $-\sigma_{\theta\theta}/\Delta T$ for the two singular points (S_1 and S_2) at the interface against the dimensionless variable w/L for $r/w = 1.0 \times 10^{-2}$ are shown in Figure 16. For $1 \geq w/L \geq 0.4$, the width of the model is not much less than the length or the height. So, the model is a simple three-dimensional structure, and does not behave like a plate structure. Therefore, the variation of the width in the range $1 \geq w/L \geq 0.4$ has little influence on the stress distribution of $-\sigma_{\theta\theta}/\Delta T$ against the variable r/w around the two singular points. For $0.2 \geq w/L \geq 0.015$, the model obviously behaves like a plate structure. Then, the stress singularity lines get close enough to raise the

magnitude of the stress field around each line. Therefore, the level of the stress distributions of $-\sigma_{\theta\theta}/\Delta T$ around the singular points, S_1 and S_2 , increases rapidly as the width w of a plate structure decreases.

4. Conclusion

In this paper, we created a three-dimensional BEM program for thermoelasticity based on Rongved's fundamental solution satisfying the boundary condition at the interface. As a result, accurate analysis using the present BEM program required less memory and was less time-consuming than BEM analysis based on Kelvin's fundamental solutions or FEM analysis. The distributions of stress singularity fields around the singular point on the stress singularity lines for dissimilar materials in three-dimensional bonded joints under thermal loading were presented and compared with the results in the previous research studies. For a uniform temperature variation applied to three-dimensional bonded joints, the stress intensity factors were proportional to the temperature variation, ΔT , and depended on the difference in the thermal expansion coefficients. Logarithmic singularity significantly influenced the characteristics of the stress distributions in three-dimensional bonded joints under thermal loading. For plate structures with very small thickness, the level of the stress distributions around the singular points on the stress singularity lines along the dimensionless distance, r/w , increased rapidly.

References

- [Barut et al. 2001] A. Barut, I. Guven, and E. Madenci, "Analysis of singular stress fields at junctions of multiple dissimilar materials under mechanical and thermal loading", *Int. J. Solids Struct.* **38**:50–51 (2001), 9077–9109.
- [Cheng et al. 2001] A. H.-D. Cheng, C. S. Chen, M. A. Golberg, and Y. F. Rashed, "BEM for thermoelasticity and elasticity with body force: a revisit", *Eng. Anal. Bound. Elem.* **25**:4–5 (2001), 377–387.
- [Cruse et al. 1977] T. A. Cruse, D. W. Snow, and R. B. Wilson, "Numerical solution in axisymmetric elasticity", *Comput. Struct.* **7**:3 (1977), 445–451.
- [Dundurs 1969] J. Dundurs, "Discussion of edge-bonded dissimilar orthogonal elastic wedges under normal and shear loading", *J. Appl. Mech. (ASME)* **36** (1969), 650–652.
- [Karami and Kuhn 1992] G. Karami and G. Kuhn, "Implementation of thermoelastic forces in boundary element analysis of elastic contact and fracture mechanics problems", *Eng. Anal. Bound. Elem.* **10**:4 (1992), 313–322.
- [Koguchi 1997] H. Koguchi, "Stress singularity analysis in three-dimensional bonded structure", *Int. J. Solids Struct.* **34**:4 (1997), 461–480.
- [Koguchi et al. 2003] H. Koguchi, M. Yamaguchi, K. Minaki, and P. Monchai, "Analysis of stress singularity fields in three-dimensional joints by three-dimensional boundary element method using fundamental solution for two-phase transversely isotropic materials", *Trans. Jpn. Soc. Mech. Eng. A* **69**:679 (2003), 585–593. In Japanese.
- [Li et al. 1992] Y. Li, H. Koguchi, and T. Yada, "Investigation of method of stress relaxation around the apex of ceramics-metal bonded structure (consideration of shape effect of apex in three dimensional dissimilar materials)", *Trans. Jpn. Soc. Mech. Eng.* **58** (1992), 1417–1423.
- [Madenci et al. 1998] E. Madenci, S. Shkarayev, and B. Sergeev, "Thermo-mechanical stresses for a triple junction of dissimilar materials: global-local finite element analysis", *Theor. Appl. Fract. Mech.* **30**:2 (1998), 103–117.
- [Munz and Yang 1992] D. Munz and Y. Y. Yang, "Stress singularities at the interface in bonded dissimilar materials under mechanical and thermal loading", *J. Appl. Mech. (ASME)* **59** (1992), 857–862.
- [Munz and Yang 1994] D. Munz and Y. Y. Yang, "Stresses near the free edge of the interface in ceramic-to-metal joints", *J. Eur. Ceram. Soc.* **13**:5 (1994), 453–460.
- [Pageau and Biggers 1995] S. S. Pageau and S. B. Biggers, Jr., "Finite element evaluation of free-edge singular stress fields in anisotropic materials", *Int. J. Numer. Methods Eng.* **38**:13 (1995), 2225–2239.

- [Prukvilailert and Koguchi 2005] M. Prukvilailert and H. Koguchi, “Stress singularity analysis around the singular point on the stress singularity line in three-dimensional joints”, *Int. J. Solids Struct.* **42**:11–12 (2005), 3059–3074.
- [Rizzo and Shippy 1977] F. J. Rizzo and D. J. Shippy, “An advanced boundary integral equation method for three-dimensional thermoelasticity”, *Int. J. Numer. Methods Eng.* **11**:11 (1977), 1753–1768.
- [Rongved 1955] L. Rongved, “Force interior to one of two joined semi-infinite solids”, pp. 1–13 in *Second Midwestern Conference on Solid Mechanics*, 1955.
- [Yamada and Okumura 1981] Y. Yamada and H. Okumura, “Analysis of local stress in composite materials by the 3-D finite element”, pp. 55–64 in *Proceedings of the Japan–U.S. Conference (Tokyo)*, 1981.
- [Yang and Munz 1995] Y. Y. Yang and D. Munz, “Stress intensity factor and stress distribution in a joint with an interface corner under thermal and mechanical loading”, *Comput. Struct.* **57**:3 (1995), 467–476.

Received 30 Jun 2006. Revised 14 Apr 2006. Accepted 30 Jun 2006.

MONCHAI PRUKVILAILERT: monchai@stn.nagaokaut.ac.jp

Department of Mechanical Engineering, Nagaoka University of Technology, 1603-1 Kamitomioka, Nagaoka 940-2188, Japan

HIDEO KOGUCHI: koguchi@mech.nagaokaut.ac.jp

Department of Mechanical Engineering, Nagaoka University of Technology, 1603-1 Kamitomioka, Nagaoka 940-2188, Japan